ISSN 1027-5495. Functional Materials, 30, No.3 (2023), p. 371-376.
doi:https://doi.org/10.15407/fm30.03.371

Multi-element vacuum-arc coatings of the TiZrHfNbTaVN system

H.Kniazieva (Postelnyk), S.Kniaziev, V.Subbotina

National Technical University "Kharkiv Polytechnical Institute",
2 Kyrpychova Str., 61002 Kharkiv, Ukraine

Received April 20, 2023

The research considers the influence of constant (U_b = −45...−200 V) and pulsed (U_{ip} = −800...−1200 V) displacement potential on the composition, structure and mechanical properties of multi-element vacuum-arc coatings of the TiZrHfNbTaVN systemX-ray diffraction analysis shows the formation of a two-phase state, which consists of an fcc crystal lattice of the NaCl structure type and a small amount of the bcc phase, which may be due to the presence of a droplet component. The use of an additional pulsed potential does not lead to an improvement in surface quality and an increase in mechanical properties. The maximum hardness of 52 GPa was obtained at a constant displacement potential of −200 V.

Keywords: multi-element coatings, nanostructure, vacuum arc method, displacement potential.

Багатоелементні вакуумно-дугові покриття системи TiZrHfNbTaVN. *Г.А.Князєва (Постільник), С.А.Князєв, В.В.Суботина*

В роботі розглянуто вплив постійного (U_b = −45...−200 V) і імпульсного (U_{ip} = −800...−1200 V) потенціалу зсуву на склад, структуру і механічні властивості багатоелементних вакуумно-дугових покриттів системи TiZrHfNbTaVN. Рентгеноструктурним аналізом показано формування двофазного стану, яке складається з ГЦК кристалічно решітки структурного типу NaCl і невеликої кількості ОЦК фази, що може бути пов'язане з наявністю крапельної складової. Застосування додаткового імпульсного потенціалу не приводить до поліпшення якості поверхні і підвищення механічних властивостей. Встановлено, що максимальна твердість 52 ГПа отримана при постійному потенціалі зсуву −200 В.

1. Introduction

The development of modern technologies requires the creation of new materials with improved properties. Recently, the attention of scientists has been attracted by multi-element coatings that have a complex of properties: increased high-temperature strength, thermal and chemical stability. Various high-performance coating technologies are used, for example, gas-plasma spraying [1] and flux-cored wire surfacing [2].

Among many known alloys [3, 4], preference is given to alloys that contain 3d transition metals in their composition. It is in these alloys that a set of improved mechanical properties can be achieved, such as hardness [5, 6], tensile strength [7, 8], malleability [9], crack resistance at low temperatures [7, 8].

Despite the fact that multi-element alloys have a complex composition, they are characterized by a fairly simple crystal structure; in most cases they have fcc and bcc crystal lattices [10–12]. Among the criteria for stabilization of a single-phase state, the configuration entropy is considered to be the main factor stabilizing the structure of a solid solution [13].

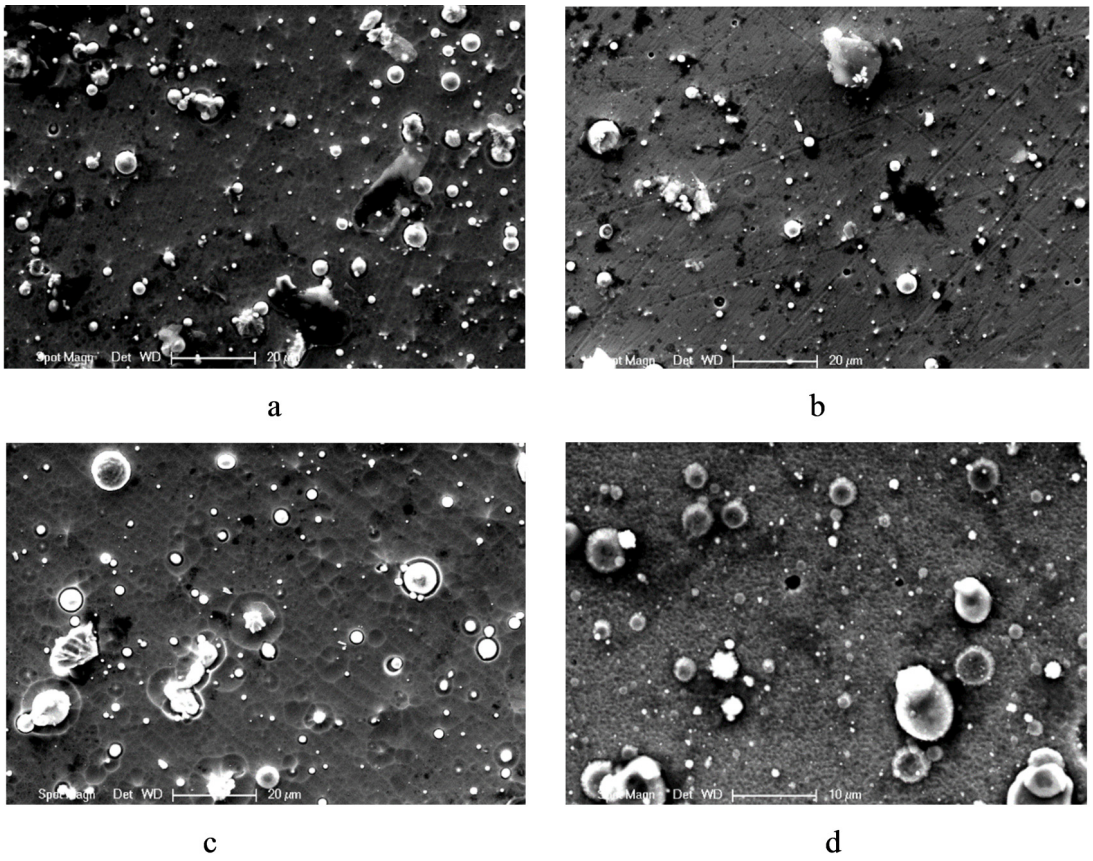

Fig. 1. Surface morphology of multi-element TiZrHfNbTaVN coatings: a — U_b = –45 V, U_{ip} = –0 V; b — U_b = –150 V, U_{ip} = –0 V; c — U_b = –150 V, U_{ip} = –800 V; d — U_b = –150 V, U_{ip} = –1200 V.

2. Samples and research methodology

To obtain a multi-element TiZrHfNbTaV coating, a cathode of this composition was fabricated by tenfold vacuum-arc remelting of a multicomponent mixture of powders of pure (purity 99.9 %) metals in a MIFI-9-3 arc furnace (in a high-purity argon atmosphere).

Multi-element coatings were deposited by the vacuum-arc method on the Bulat-6 installation at a constant nitrogen atmosphere pressure of $7 \cdot 10^{-4}$ Torr at various applied bias potentials: the constant bias potential varied from –45 V to –200 V, the bias pulse potential was –800 V and –1200 V. The deposition time was 1.5...2 hours. Before deposition, the samples were subjected to ion cleaning and activation of the substrate surface by bombardment with metal ions included in the coating; a negative potential of –1300 V was applied to the substrate for 10...15 minutes.

The surface morphology was studied using a Philips XL 30 ESEM scanning electron microscope with a built-in EDX energy-dispersive X-ray detector. The elemental composition was determined by the X-ray fluorescence method using an apparatus of the "SPRUT" series.

X-ray diffraction analysis was carried out on a DRON-4 diffractometer in copper radiation in the angular range $2\theta = 20...90°$ with a scanning step of 0.01°, exposure time 10 sec. The measurements were carried out according to the θ–2θ scanning scheme with Bragg-Brentano focusing.

To interpret X-ray diffraction patterns, Tables of the International Center for Diffraction Data [14] with powder diffraction files (JCPDS) were used. The size of crystallites and the value of microdeformation were calculated by the approximation method [15].

Hardness measurements were carried out on hardness testers PMT-3 (load 10–200 g, holding time 30 s) and Mikron-Gamma (load within 0.5 N, with automatic loading and unloading). To obtain reliable data, 10 measurements were carried out for each sample. The resulting indentation depth did

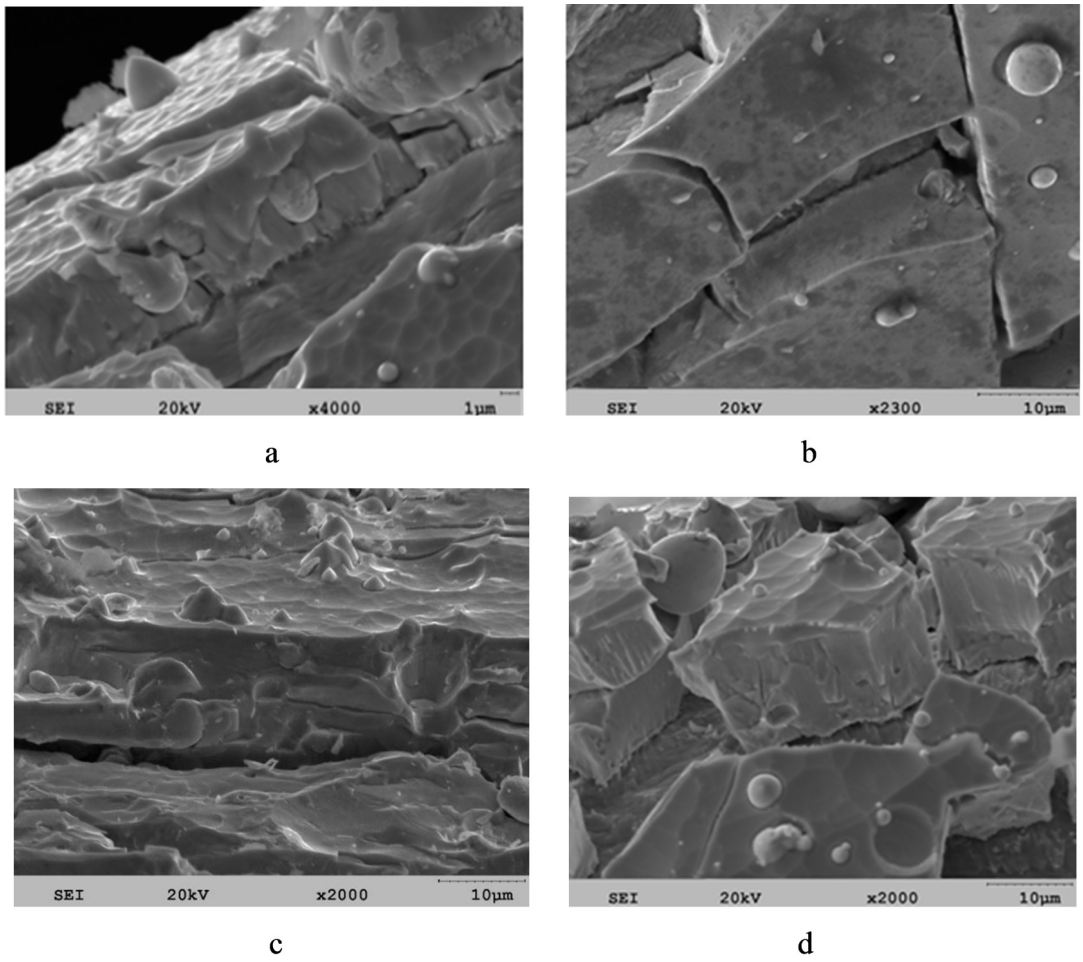

Fig. 2. Morphology of the side surface of multi-element TiZrHfNbTaVN coatings: a — U_b = –45 V, U_{ip} = –0 V; b — U_b = –150 V, U_{ip} = –0 V, c — U_b = –150 V, U_{ip} = –800 V; d — U_b = –150 V, U_{ip} = –1200 V.

not exceed 10 % of the total coating thickness, which minimizes the effect of the substrate.

3. Results and discussions

The surface morphology of multi-element TiZrHfNbTaVN coatings is shown in Fig. 1 with a slight magnification. It can be seen that the coating surface is inhomogeneous, there is a droplet component, the amount of which decreases with increasing bias potential. An additional supply of a pulsed potential leads to a decrease in the amount of the droplet phase, but the average size of droplets is slightly increased. In order to reveal the presence of a droplet phase inside the coating itself, an additional study of the side surface was carried out at a higher magnification (Fig. 2), which showed that there is no droplet component inside the coating itself. The elemental composition of the coating is presented in Table 1.

An analysis of the elemental composition of the TiZrHfNbTaVN coatings with a change in the bias potential in a constant mode showed that most of the elements in the multicomponent coating system have stable values of the mass fraction. A change in the bias potential in given intervals, as well as the use of a pulsed bias potential leads to some change in the composition of titanium, vanadium, and hafnium. Of particular note is the presence of an insignificant amount of vanadium in the multicomponent system.

The composition of the droplet was additionally studied. Fig. 3 shows an image of a drop (at high magnification) and an energy-dispersive spectrum, the elemental composition of which is presented in Table 2. The elemental composition of the droplets (Table 2) does not change, but is characterized by a decrease in the amount of Ti, Hf, Ta due

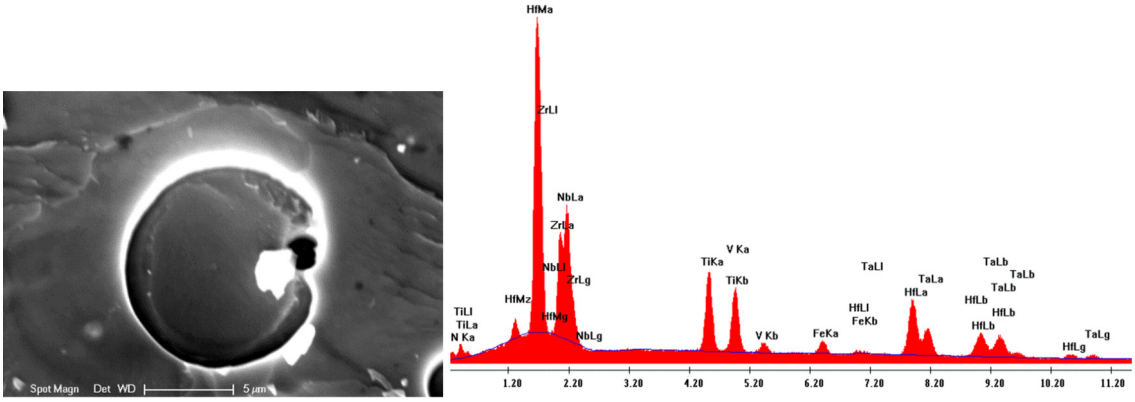

a b

Fig.3. Image (a) and energy dispersive spectrum (b) of a drop: a — without impulse potential; b — at constant Ub=−150V, 1 — Ub=−45V, 2 — Ub=−75V, 3 — Ub=−150V, 4 — Ub=−200V, 5 — Uip=−800V, 6 — Uip=−1200V.

Table 1. Elemental composition of the TiZrHfNbTaVN coating

Deposition mode		Elemental composition, wt. %					
U_b, V	U_{ip}, V	Ti	Zr	Hf	Nb	Ta	V
Without impulse stimulation							
−45	0	17.97	13.64	34.50	11.64	21.92	0.33
−75		20.20	13.60	32.43	11.61	21.66	0.50
−150		17.46	13.72	34.12	11.83	22.62	0.25
−200		18.24	12.47	37.09	12.93	17.89	1.38
With impulse stimulation							
−150	−800	24.14	11.18	33.18	13.19	14.18	4.13
	−1200	20.10	12.25	35.14	14.02	15.44	3.05

to an increase in Zr and Nb. The kinetic energy of Zr and Nb ions is 116 eV that is the highest among all the participating elements [16], and they have the smallest distribution radius over the surface. Thus, conditions are created for the condensation of these elements in certain local areas of the surface. The appearance of Fe is associated with "parasitic" dusting from the back side of the sample of the substrate material. The increased concentration of nitrogen is explained by a relatively low ionization of this element and local saturation of the droplet material as a result of active adsorption of the developed interface of the microformation. These changes in the composition cause the formation of a solid solution based on the bcc lattice, in contrast to the main coating material.

The X-ray diffraction spectra of the TiZrHfNbTaVN coatings obtained at different bias potentials are shown in Fig. 4. X-ray diffraction analysis shows that the coating

Table 2. Elemental composition of the drop

Elemental composition, wt. %							
Ti	Zr	Hf	Nb	Ta	V	Fe	N
5.82	23.22	24.35	25.04	12.69	4.03	1.31	3.55

consists of crystallites with an fcc crystal lattice of the NaCl structural type and a small amount of bcc phase, which can be due to the presence of a droplet component. During deposition in the regime without pulsed stimulation, the orientation of crystallite growth with the (111) axis is predominant. When an additional pulsed potential is applied, the preferential orientation changes to (200). Broad lines in the diffraction patterns indicate a high dispersion of crystallites.

Calculations showed that the size of crystallites is in the nanorange of 15...90 nm. The bias potential of −75 V provides the lowest level of microstrains. The mode U_b =

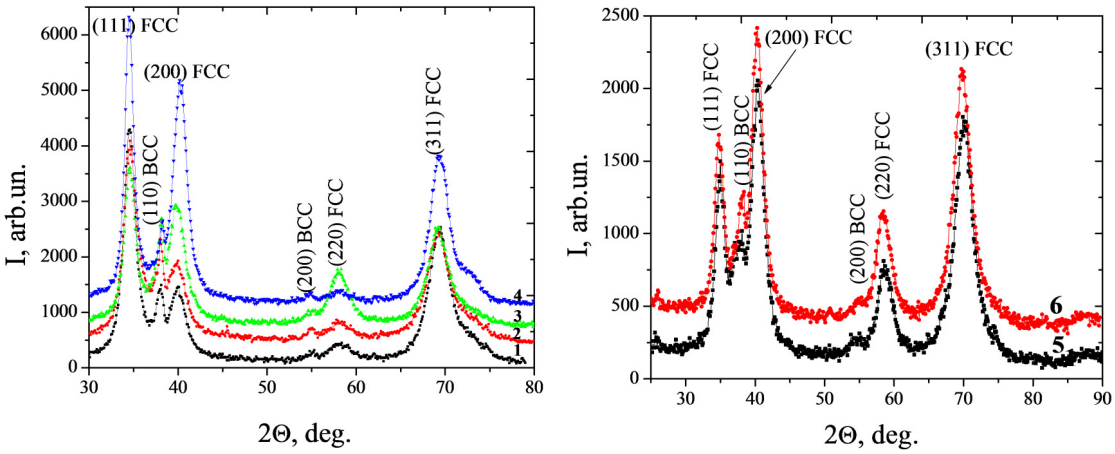

Fig.4. Sections of X-ray diffraction spectra of TiZrHfNbTaVN coatings depending on the bias potential. a — macrostructure of the sample, b — appearance of the imprint during microindentation, c — local destruction.

−45 V ensures the formation of the smallest crystallites of 15 nm at relatively low levels of microstrain of 1.15 %. The use of a pulsed potential did not reduce the crystallite size below 15 nm, while the level of microstrains somewhat increases.

The measured microhardness of the samples showed that in the pulseless mode, the microhardness is about 37833 MPa, with pulsed action U_{ip} = −800 V — 27796 MPa, and with U_{ip} = −1200 V — 23573 MPa. Also, in order to obtain reliable data, the nanohardness was additionally measured, which showed that at a constant potential up to −150 V, the nanohardness is ≈ 34 GPa, and at −200 V, this is 52 GPa; applying a pulsed potential leads to a drop in the average hardness value of ≈24 GPa.

Macroscopic analysis of the surface of the samples showed that there is a network of macrocracks on the surface (Fig. 5), which are the result of fracture due to a high level of stress. At the same time, the absence of a microcrack during indentation does not exclude the working capacity of such a coating. In general, microhardness data correlate with nanohardness data and the test conditions are more approximate to conditions of high contact loads in real parts.

As can be seen from the measured values of micro- and nanohardness, the use of a pulsed potential does not lead to an increase in hardness above 30 GPa. At the same time, the deposition of a multi-element coating without a pulsed potential makes it possible to provide a hardness level from 33 to 52 GPa. The hardness of 52 GPa, obtained at a potential of −200 V, is provided mainly by an increased level of microstrains. The reduced hardness on the samples obtained with the practice of a pulsed potential can be explained by microbrittle fracture when applying a local load, which is well illustrated in Fig. 5b.

4. Conclusions

In the work it was established that the multi-element coatings of the TiZrHfNbTaVN system have an fcc crystal lattice of the NaCl structural type and a small amount of bcc phase, which can be due to the presence of a droplet component. It is shown that the coating structure does not contain a nitride component with a complex chemical compound lattice, and the structure is based only on a multicomponent solid solution. The additional use of the pulsed potential does not lead to an improvement in the quality of the surface and an increase in the mechanical characteristics, which may be due to the formation of a highly stressed state leading to cracking. Applying a constant bias potential of −200 V makes it possible to achieve a coating hardness of 52 GPa.

References

1. D.B.Hlushkova, V.A.Bagrov, S.V.Demchenko et al., *Problems of Atomic Science and Technology*, **4**, 125 (2022).
2. B.Trembach, O.Balenko, V.Davydov et al., IEEE 4th International Conference on Modern Electrical and Energy System (MEES) (2022), p.01.
3. M.G.Poletti, L.Battezzati, *Acta Materialia*, **75**, 297 (2014).

a b

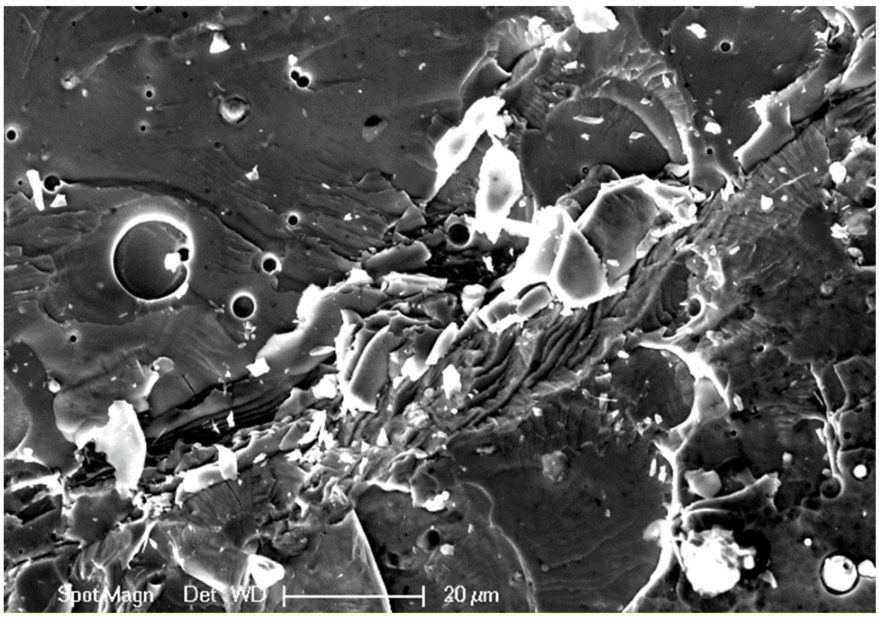

c

Fig.5. The state of the sample surface at Uip=−800V, an example of an imprint when measuring microhardness, as well as the place of local destruction.

4. F.Tian, L.K.Varga, N.Chen et al., *Intermetallics*, **58**, 1 (2015).
5. J.Zaddach, C.Niu, C.C.Koch, D.L.Irving, *JOM*, **65**, 1780 (2013).
6. G.Salishchev, M.Tikhonovsky, D.Shaysultanov et al., *Journal of Alloys and Compounds*, **591**, 11 (2014).
7. B.Gludovatz, A.Hohenwarter, D.Catoor et al., *Science*, **345**, 1153 (2014).
8. A.Gali, E.George, *Intermetallics*, **39**, 74 (2013).
9. F.Otto, Y.Yang, H.Bei, E.George, *Acta Materialia*, **61**, 2628 (2013).
10. O.V.Sobol', A.A.Andreev, V.F.Gorban' et al., *Journal of Nano- and Electronic Physics*, **10**, 05046 (2018).
11. S.Gorsse, M.H.Nguyen, O.N.Senkov, D.B.Miracle, *Data in Brief*, **21**, 2664 (2018).
12. O.V.Sobol', A.A.Postelnyk, R.P.Mygushchenko et al., *Journal of Nano- and Electronic Physics*, **10**, 02035 (2018).
13. Y.Zhang, T.T.Zuo, Z.Tang et al., *Progress in Materials Science*, **61**, 1 (2014).
14. http://www.icdd.com
15. A.S.Rusakov, Rentgenografiya Metallov, Atomizdat, Moscow (1977).
16. G.Yu.Yushkov, A.Anders, E.M.Oks, I.G.Brown, *Journal of Applied Physics*, **88**, 5618 (2000).